Two-wavelength digital holographic interferometry for unambiguous range extended measurements in fluid mechanics

Gramoz Çubreli[1,2*], *Pavel* Psota[2], *Ahmad* Kouta[1], and *Petra* Dančová[1]

[1]Faculty of Mechanical Engineering, Technical University of Liberec, Studentská 2, 461 17 Liberec 1, Czech Republic
[2]Faculty of Mechatronics, Informatics and Interdisciplinary Studies, Technical University of Liberec, Studentská 2, 461 17 Liberec 1, Czech Republic

Abstract. Non-contact optical methods such as digital holographic interferometry are highly suitable in measurements where the phenomena is fast, performed in transparent or semi-transparent environment and mustn't be obstructed as when applying local contact techniques. Such specific application can be studying dynamic events during transonic and supersonic blade flutter. Fast, sensitive and rather easy access to the phase information make these techniques very attractive in the study of phase objects/phenomena. However, since light's phase is bounded to a repetitive cycle of 2π radians, the range of measurement is limited to one cycle of the phase, limiting applications to small gradient phenomena. This paper presents a new interesting way of by-passing this limitation, while still keeping noise values low, by introducing a second laser with a close value wavelength, giving rise to a new interferometric pattern with an extended unambiguous range of measurement. Image acquisition is done simultaneously for both wavelengths and all reconstructions are digitally performed. The principle and preliminary results are included in this paper.

1 Introduction

For fast occurring phenomena, where the nature and properties of the fluid must be studied without disturbances from the observer, non-contact optical methods such as digital holographic interferometry present themselves as reliable, fast and accurate techniques. Such technique require nonetheless that the liquid under study to be transparent or semi-transparent, in order for the optical rays to pass through and be recorded. Phase imaging holographic interferometry provides high flexibility and means for highly sensitive measurement of phenomena with optical path variations.

Interferometric methods offer very high precision measurements which lie in the range of the nanometric scale [1]. One clear advantage is the fast numerical reconstruction.

Digital holographic interferometry is being used more and more due to its clear advantages over the conventional holographic technique. Probably the most important advantage lays in its power to acquire and process images/information in real time. It offers the possibility of easily acquiring images through CCD cameras, complex and fast numerical processing, storage of large data, numerical image reconstruction and real time presentation of the phenomena. Digital holographic interferometry finds a very wide range of applications, notably in medical imaging where the study of biological specimens has been made easier and better. The range of application is quite wide, in industrial and scientific applications, notably in quality control in micro-electro-mechanical systems (MEMS) fabrication, ultraprecise manufacture, research in ophthalmology etc. [2]

In this paper, an off-axis two-wavelength digital holographic interferometry technique for resolving the issue of phase unwrap ambiguity for the case of a resistor is presented.

When the object we measure has sudden profile changes that go beyond the range limit allowed for a specific wavelength, a phase ambiguity arises. If this ambiguity isn't solved in the phase unwrapping process, it will give faulty result, not mapping the true profile of the phenomenon we are looking at. The phase is proportional to the surface profile (when trying to image surface profiles from reflection), to the integral of the refractive index for transparent media, otherwise it is linked to the wavelength via respective formula. [3]
Two-wavelength interferometry offers an alternative solution to solve the phase ambiguity problem. [3]

This method enables a fast and efficient way of imaging the phase profile for a multitude of applications. It makes it possible to measure in real time phenomena that cause large phase changes without ambiguity. Thus, by using two lasers or more, the range of unambiguity can be increased compared to using a single laser [1]. The disadvantage of this technique is that any noise present in the phase profile of any of the wavelengths will get amplified by a magnification factor equal to one of the synthetic wavelength [4]. Off-axis configuration spatially separates the holographic images away from the undiffracted zero order. [5,6]

* Corresponding author: Gramoz Çubreli gramoz.cubreli@tul.cz

Two-wavelength interferometry can be used in many areas of optical metrology, such as for the measurement of the thickness and surface profile/inspections of objects [3]. It can be used in research dealing with samples having large topographical changes and biological samples [7].

Due to its extended unambiguity range, high-speed acquiring and large field of view, the method will be applied for investigation of high-speed flow in planar blade cascades, namely for studying dynamic events during transonic and supersonic blade flutter.

In interferometry, specifically phase-shifting interferometry, at least three intensity maps are needed to resolve the phase map, while in two-wavelength interferometry it is six but can be decreased to two. [8]

2 Principle of two-wavelength interferometry

In single-wavelength technique, when the object of investigation is thicker than the laser wavelength (in our case the temperature range that can be mapped surpasses the range of measurement) used for research, the phase gets wrapped and suffers from 2π ambiguities. The range of measurement is directly connected to the wavelength. For smaller wavelengths, the range decreases, while for longer wavelengths it increases [4]. Longer wavelengths produce fewer fringes, reducing the number of 2π ambiguities [9]. Phase has a periodicity of 2π radians and the phase of light can be expressed as a multiple of this 2π periodicity. The repetitive nature of light propagation as wave in the form of a sinusoidal wave makes the range of clear unambiguous measurement to be limited to one cycle of repetition, i.e. one wavelength. Due to Nyquist criteria, the real range of unambiguity is limited to a half-wavelength [10]. In other words, the wrapping is a direct consequence of the 2π periodicity of the $arctan$ function used to extract the phase profile from the light that is being measured [4,11]. During the phase unwrapping process, the absolute phase difference between points of measurement in time and space must be less than the value of π radians for a better unwrapping [12]. There are cases when the difference is much higher, causing multiple wrapping simultaneously. Care must be taken when dealing with such situations.

The sole idea of using a two-wavelength technique comes from the limitations mentioned above. In two-wavelength or multiple-wavelength interferometry, the unambiguous range of measurements gets extended by what is called the synthetic wavelength [1,11]. The general graphical concept representation is shown in the following fig.1.

A requirement that must be fulfilled for such optical technique is that the optical path from all beams must be the same. This condition can create some difficulties in the building of the optical setup, and sometimes it can turn out to be expensive [2]. Hence, appropriate geometrical setup must be found in order to accommodate this condition.

A disadvantage of this technique is that, despite ambiguity being solved (reduced), the range of unambiguous measurement can be extended at the cost of increasing noise by the factor of the ratio between the synthetic/equivalent wavelength and the shortest wavelength Λ_{eq}/λ_1, thus decreasing the sensitivity of the technique for the same factor. In length measurement, this is reflected as increase of uncertainty measurement. [1,4]

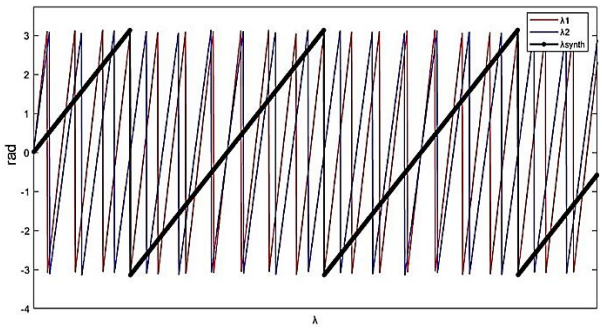

Fig.1. Graphical representation of the difference of the measurement range covered by smaller (λ_1, λ_2) and larger (λ_{synth}) wavelength. [9]

Let the change in refractive index that the wave experiences while passing through a heat field be expressed as $\varphi(x, y)$, then the interference pattern on the CCD camera is proportional to:

$$I(x,y) \sim \cos\left[2\pi\varphi(x,y)\left(\frac{1}{\lambda_1}-\frac{1}{\lambda_2}\right)\right] \quad (1)$$

, which leads to what is called the synthetic wavelength (or equivalent/beat wavelength) [13,14]:

$$\frac{1}{\Lambda_{eq}}=\frac{1}{\lambda_1}-\frac{1}{\lambda_2}=\frac{\lambda_2-\lambda_1}{\lambda_1\lambda_2}\Rightarrow\Lambda_{eq}=\Lambda_{12}=\frac{\lambda_1\lambda_2}{|\lambda_2-\lambda_1|} \quad (2)$$

From (2), it can be seen that the smaller the difference in the dominator, the larger the synthetic wavelength will be. This implies that, if the two lasers have a smaller difference in wavelengths, then the new range of unambiguous measurement will increase. [5,9]

For the case of multiple-wavelength interferometry, the synthetic wavelength can be defined as [15,6]:

$$\Lambda_{eq}=\frac{\lambda_1\lambda_n}{|\lambda_n-\lambda_1|} \quad (3)$$

, where subscript n represents the number of lasers used.

3 Unwrapping

Phase unwrapping has been extensively studied and adapted for many different applications. Different techniques that require phase unwrapping process are magnetic resonance [16], x-ray crystallography [17], synthetic aperture radar (SAR) [18] etc.

There exist many different techniques to extract the phase distribution from the fringe pattern, such as phase-shifting profilometry, Fourier transform profilometry, windowed Fourier transform profilometry etc. Highest resolution and accuracy are provided through the first

technique, phase-shifting profilometry [19]. Phase-shifting interferometry is not suitable for measuring dynamic phenomena because it requires at least three holograms to be recorded in order to solve the equations to retrieve the coefficients [11].

Phase unwrapping process has some requirements when it comes to the noise and the discontinuity the phase might have. The easiest way is usually to use one of the 2π phase unwrapping algorithms, but in certain cases not the same algorithms are valid for different kinds of wrappings. Unwrapping algorithms usually are heavy computational wise and can be subject of failure where the object or phenomena under study has large irregularities.

In the cases when the phenomena is restricted to a small confinement in the image, the edge of the image where no change has occurred can be chosen as the starting point for phase unwrapping, since interferometric measurement require at least one point where the phase change is known. [11]

The basic idea of phase unwrapping consists on dividing the phase image into horizontal line, which are then unwrapped pixel by pixel by adding or subtracting the offset (2π radians) when necessary. This is done separately for each of the lines. Once this is done, the same process happens, but vertically. At the end the phase image will be unwrapped in 2D [12].

By having the difference of the two wrapped phase profiles created from both wavelengths, a new wrapped phase profile arises. This new phase profile ''belongs'' to a much greater wavelength, which we called previously as the synthetic wavelength. The synthetic wavelength is used to resolve the ambiguity by detecting the average phase shift (by calculating the fringe order) while using the lower laser wavelength to measure the temperature.

Based on the dependence of the path, there are path dependent and path independent phase unwrapping techniques. In path dependent techniques, image processing is used to detect the edges and the phase ambiguities, and from that to calculate the offset that must be added or subtracted, while in path independent techniques the regions where error could be caused are eliminated before the phase unwrap process starts. [9]

Spatial phase unwrapping, from its name, uses the relationship between the phase information of the spatial neighboring pixels [19,20]. There exist different kinds of spatial unwrapping algorithms, notably the Goldstein's method, Flynns' method etc.

Determining the fringe order from spatial neighboring pixels is not possible in the spatial phase unwrapping since it is based on the information that neighboring pixels have.

The necessity of temporal phase unwrapping plays in when we need to unwrap a general phase map with large discontinuities. The fact that each pixel is unwrapped independently from its neighbor makes that any present noise in one of the pixels not to spread to other pixels during the process of unwrapping. There are also different kinds of temporal phase unwrapping algorithms, and the advantage of using temporal unwrapping stands from the fact that phenomena with large phase changes (in the case of profile measurements coming from high discontinuities) can be studied. The simplest one is the Gray-code temporal phase unwrapping. Other techniques, for example that use additional wrapped phase maps that differ from their fringe order to unwrap temporally the phase map, can be categorized into three groups: multiwavelength (heterodyne), multifrequency (hierarchical) and number-theoretical approach. A detailed review over these three techniques has been published, according to which, this group outperforms the Gray-code algorithm in accuracy, pattern efficiency and unambiguous range. [8]

The interference pattern on the CCD camera can also be expressed as [11,10]:

$$\begin{aligned} I(x,y) &= A(x,y) + \\ &+ \sum_{l=1}^{2} B_l(x,y)\cos\{\varphi_l(x,y) + 2\pi f_l x\} = \\ &= A(x,y) + \\ &\quad + B_1(x,y)\cos\{\varphi_1(x,y) + 2\pi f_1 x + 2\pi f_1 y\} + \\ &\quad + B_2(x,y)\cos\{\varphi_2(x,y) + 2\pi f_2 x + 2\pi f_2 y\} \end{aligned} \tag{4}$$

, where $A(x,y)$ is the background intensity and pattern brightness, $B(x,y)$ is the intensity modulation and f_1, f_2 are the carrier frequencies. This is known as spatial carrier frequency interferometry. The relation between the interference phase and the refractive index variation is given in (5). If we assume no variation of the refractive index n in the direction of propagation, then the integral simplifies in multiplication only:

$$\varphi(x,y) = \frac{2\pi}{\lambda}\int_L \Delta n(x,y,z)ds = \frac{2\pi}{\lambda}\Delta n(x,y)L \tag{5}$$

, where ds denotes the differential distance along the line of integration L. The wrapped phase is extracted by:

$$\varphi(x,y) = \arg\{I(x,y)\} = \arctan\left(\frac{Im\{I(x,y)\}}{Re\{I(x,y)\}}\right) \tag{6}$$

The basic idea of unwrapping consists of shifting back to its place each phase jump by adding or subtracting integer multiples of 2π radians, in order to draw the phase as a continuous function (without the jumps, causing this characteristic sawtooth/triangle form of the phase), which can be expressed as:

$$\theta(x,y) = \varphi(x,y) + 2\pi N(x,y) \tag{7}$$

The main idea is to retrieve as fast and accurately possible the fringe order term $N(x,y)$ for each of the pixels of the camera. We can make of use the extended range of unambiguous measurement from the synthetic wavelength and the accurate measurement of single wavelength phase that doesn't suffer from noise amplification to unwrap the original phase profile. There are several ways of how to do it and different technique corresponding to different applications. The most straightforward way of unwrapping is to make use of the synthetic phase profile in order to extract the average

phase shift (fringe order). By making use of the average operator ⟨ ⟩ the procedure can be mathematically represented as:

$$N = round\left(\frac{\langle\varphi_{synth}\frac{\Lambda_{eq}}{\lambda_2}\rangle - \langle\varphi_2\rangle}{2\pi}\right) \quad (8)$$

Other unwrapping procedures are for example the hierarchical temporal phase unwrapping which uses one of the wavelength's phase map, usually the one with the shortest wavelength. It unwraps the phase map with the help of additional wrapped phase maps which have different fringe orders. Temporal processing is for relatively slowly developing phenomena.

It is worth saying that, for any kind of phase unwrapping algorithm, if the process is successful, the final accuracy will be identical. The difference between hierarchical and multiwavelength unwrapping lays in that that the first uses one of the wavelengths for the process of unwrap, while the later uses the synthetic wavelength to start the process of unwrapping. [14]

The information that was measured from both wavelengths is retrieved in the reconstructed phase field. Both phase information have different dimensions in the Fourier spectrum, thus they must be cropped and resized in order to be used for the obtention of the synthetic phase field. This means that the size of pixels in both fields must be the same. This is achieved by resizing one of the phase fields, using the equation:

$$\Delta\xi_2' = \frac{\lambda_1}{\lambda_2}\Delta\xi_2 \quad (9)$$

, where $\Delta\xi_2$ denotes the sampling interval before compensation. Linear interpolation between neighbouring pixel values is adopted to determine the value of the compensated pixel.

4 Optical setup

Fig.2. represents the experimental lensless Fourier optical setup used to conduct this experiment. Two fiber coupled DFB (distributed feedback) laser diodes having different wavelengths are used. Light is split into the reference (RB1, RB2) and object beams (OB1, OB2) by means of fibersplitters. The object beams are combined and are collimated by a lens to then fall onto the diffuser. Scattered light from the diffuser passes through the measured area (MA) to combine with reference beams and be recorded by the camera (CAM). Both reference beams form angles with respect to the axis of propagation. It is these angles that introduce the spatial carrier frequencies that make it possible to separate phase information.

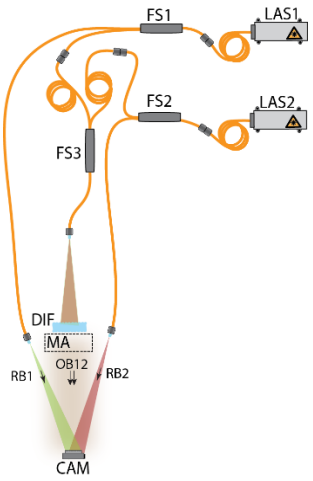

Fig.2. The two-wavelength lensless measuring system: LAS-laser, FS-fiber splitter, DIF-diffuser, MA-measured area, OB-object of investigation, RB-reference beam, CAM-camera .

Two lasers of wavelengths $\lambda_1 = 773nm$ and $\lambda_2 = 780nm$ were employed for the measurement.

According to (2), this gives rise to a synthetic wavelength of $\Lambda_{eq} = 86134.28nm$

5 Results and discussion

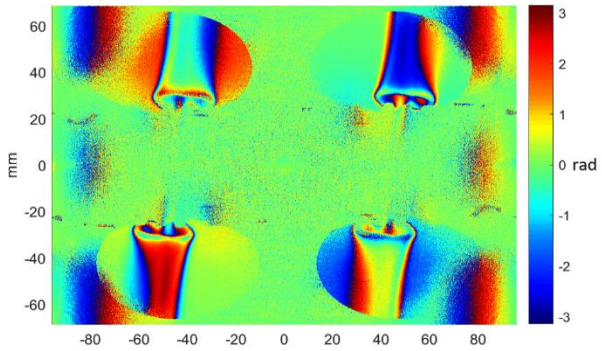

Fig.3. Reconstructed phase field map at some time instant.

Fig.3. represents the reconstructed phase field map recorded by the CCD camera at some time instant. Each recorded phase field is represented in a conjugated pair. The introduction of spatial carriers through the introduction of the angle between each of the reference wave and the axis of propagation has introduced enough separation so that the set of conjugated phase pairs don't overlap and can be filtered out confidently (i.e. off-axis arrangement). Any of the identical but conjugated pair carries the same valuable phase information used for further analysis. Any sudden change of the color red-blue indicates a 2π jump.

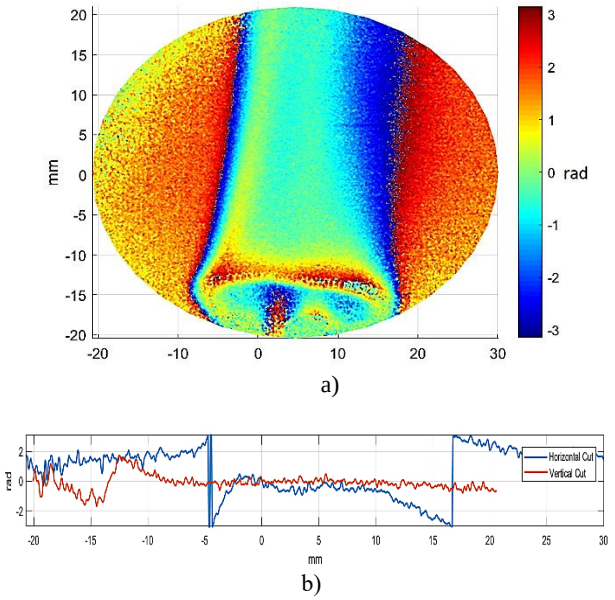

Fig.4. a) Reconstructed phase field map at some time instant from λ_1 and b) plot of the phase profile run across the phase field horizontally and vertically through the origin axis.

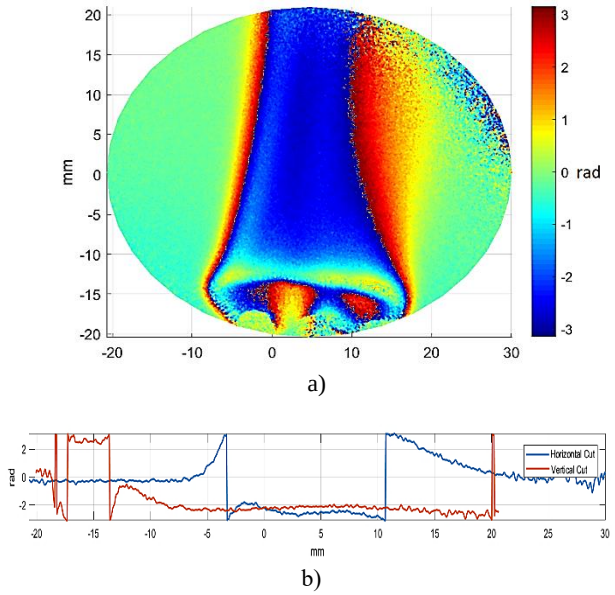

Fig.5. a) Reconstructed phase field map at some time instant from λ_2 and b) plot of the phase profile run across the phase field horizontally and vertically through the origin axis.

Fig.4. and fig.5. represent the reconstructed phase field map for each of the wavelengths. The background is masked out and only the physical field of view is shown. For different wavelengths, the camera "sees" different phase values, thus making the profile look different as what is seen from the other wavelength. The phase profile was plotted for both phase field maps, passing by the origin axis for both horizontal and vertical profiles. Clear phase jumps can be seen in the horizontal cut of fig.4. as indicated in fig.4.b) while the phase profile across the vertical cut of the phase field is smoother and no noticeable jump can be observed.

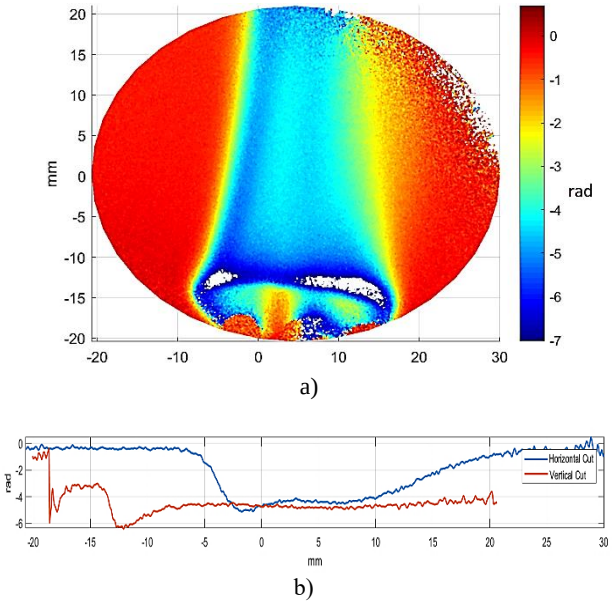

Fig.6. a) Corrected phase field map at some time instant from λ_2 and b) plot of the phase profile run across the phase field horizontally and vertically through the origin axis

Fig.6. represents the corrected phase map coming from λ_2 based on (7). The phase field that had 2π jumps is now corrected and represents visually a continuous phase map.

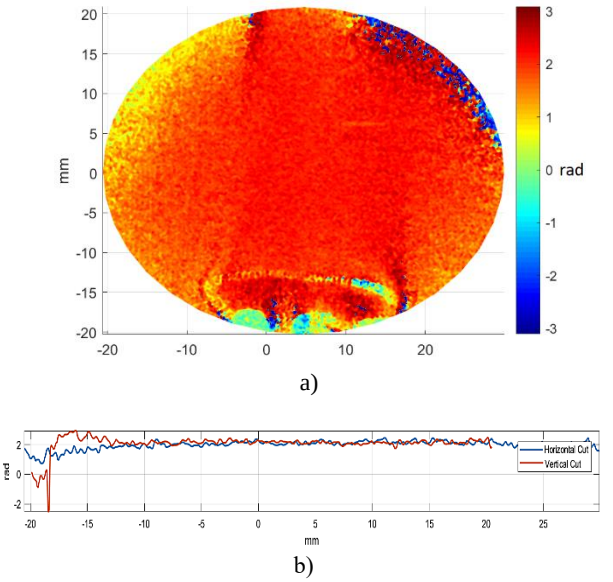

Fig.7. a) Synthetic phase field map at some time instant and b) phase profile run across the phase field.

Fig.7. represents the fictional synthetic phase map which the CCD camera would have "seen" if a laser with wavelength Λ_{eq} would have been used. In our case, since the heat gradient wasn't high, the synthetic phase map manifests itself with relatively smooth flat profile. It is worth noting that even the synthetic phase map can present phase jumps if the range of measurement is exceeded. The synthetic phase map however obscures phenomena that cause relatively small phase changes.

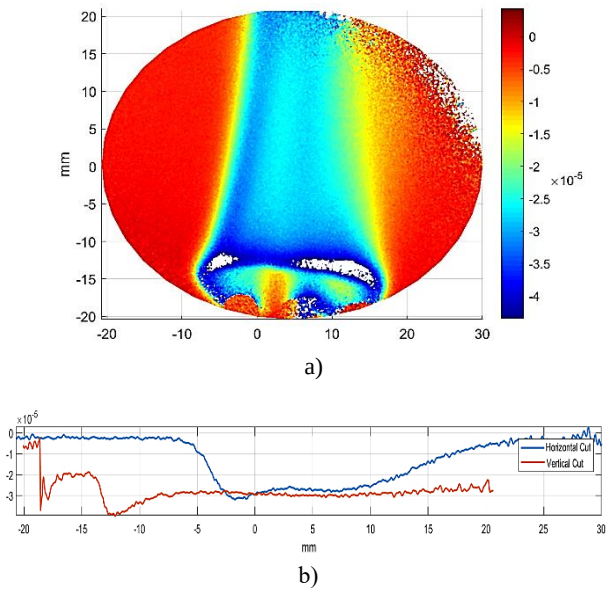

Fig.8. a) Refractive index field map at some time instant and b) refractive index profile run across the field.

Through the phase field map of either λ_1 or λ_2, the refrative index distribution can be obtained via (5) assuming a 2D distribution field of the refractive index. A distribution of the refractive index at some instant is shown in fig.8. Notice that digital holographic interferometry is able to detect very small changes in the refractive index cause by external influence (in this case heat gradient).

Through the determination of the refractive index, many other important parameters such as the temperature, density, fluid velocity etc. can be determined. This allows for the study of fluid and gases and phenomena related to. An interesting application of such technique could prove useful for the study of shockwaves around blade cascade in wind tunnels. Flow in wind tunnels are supersonic and demonstrate high levels of pressure and velocities. Such high gradients cause many fold wrapping of the phase. The use of a two-wavelength technique could therefore help in studying e.g. dynamic events during transonic and supersonic blade flutter.

Fig.9. represents the temperature change field calculated by making use of λ_2. It was calculated using the following mathematical relation :

$$T(x,y) = \frac{\lambda_2 \cdot \varphi(x,y)}{2\pi L \frac{dn}{dT}} \tag{10}$$

, where $L = 20mm$ is the estimated object length and $\frac{dn}{dT} = -0.9617 \cdot 10^{-6}\ °C^{-1}$ [15] is the change of refractive index per unit temperature.

But, this temperature was measured as a reference to the starting temperature $T_0 = 20°C$ in our case. Thus, the absolute temperature can be calculated as:

$$T_{abs}(x,y) = T_0 + T(x,y) \tag{11}$$

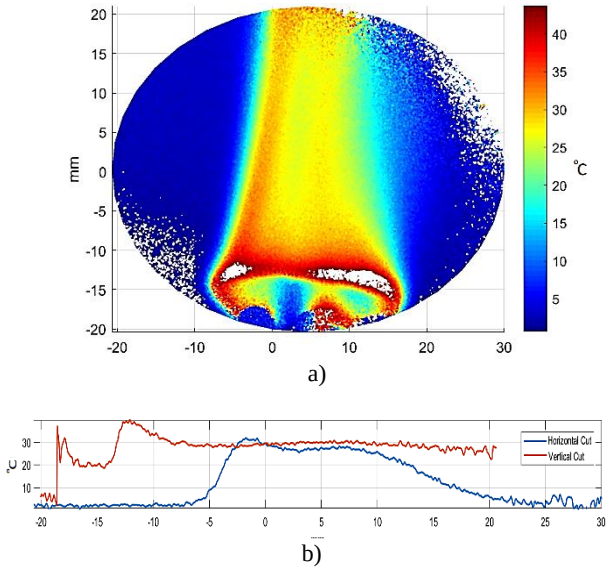

Fig.9. a) Reconstructed temperature field map $T(x,y)$ at some time instant and b) temperature profile run across the field.

6 Conclusions

This paper introduces a new approach to measure dynamic processes in fluid mechanics using lensless Fourier digital holographic interferometry with extended dynamic range. The investigation specifically deals with measuring the temperature field created from a resistor. The temperature is estimated through the optical phase, which was captured by a CCD camera. The captured phase is wrapped due to 2π limitations coming from the bounded nature of light and the two-wavelength technique deals in solving the phase ambiguity and determining the absolute phase values.

A key factor in this investigation is the use of two wavelengths and the recording of digital holograms from both wavelengths in one shot. We showed that the spectral separation of the phase information from both wavelengths can be achieved when the hardware of the experimental arrangement (angles of the reference waves) is properly adjusted [11]. The difference between the measured phase fields yields in a synthetic phase that has significantly larger dynamic range of measurement [21]. Such range covers large changes of the measured quantity as it was demonstrated in our investigation. However, the synthetic phase is more influenced by noise. By combining the synthetic phase and the phase obtained from the single wavelength, we can achieve the same accuracy as single wavelength technique but with a significantly higher range of measurement. This method is applicable to dynamic processes in fluid mechanics and could be applied for further studies of dynamic events during transonic and supersonic blade flutter in wind tunnels.

The advantages of such technique are its simplicity, fast acquisition, processing and displaying results, even in real time and in combination with the two-wavelength technique the unambiguous range of measurement is considerably increased without amplifying the noise.

Acknowledgment

This research was supported by the Ministry of Education, Youth and Sports of the Czech Republic – program Inter-Excellence, project No. LTAUSA19036.

References

[1] Meiners-Hagen, K., Schödel, R., Pollinger, F. & Abou-Zeid, A. Multi-wavelength interferometry for length measurements using diode lasers. *Meas. Sci. Rev.* **9**, 16–26 (2009).

[2] Guo, T., Li, F., Chen, J., Fu, X. & Hu, X. Multi-wavelength phase-shifting interferometry for micro-structures measurement based on color image processing in white light interference. *Opt. Lasers Eng.* **82**, 41–47 (2016).

[3] Turko, N. A., Eravuchira, P. J., Barnea, I. & Shaked, N. T. Simultaneous three-wavelength unwrapping using external digital holographic multiplexing module. *Opt. Lett. Vol. 43, Issue 9, pp. 1943-1946* **43**, 1943–1946 (2018).

[4] Turko, N. A. & Shaked, N. T. Simultaneous two-wavelength phase unwrapping using an external module for multiplexing off-axis holography. *Opt. Lett.* **42**, 73–76 (2017).

[5] Parshall, D. & Kim, M. K. Digital holographic microscopy with dual-wavelength phase unwrapping. *Appl. Opt. Vol. 45, Issue 3, pp. 451-459* **45**, 451–459 (2006).

[6] Jaedicke, V. *et al.* Multiwavelength phase unwrapping and aberration correction using depth filtered digital holography. *Opt. Lett.* **39**, 4160–4163 (2014).

[7] Khmaladze, A., Kim, M. & Lo, C.-M. Phase imaging of cells by simultaneous dual-wavelength reflection digital holography. *Opt. Express* **16**, 10900 (2008).

[8] Zuo, C., Huang, L., Zhang, M., Chen, Q. & Asundi, A. Temporal phase unwrapping algorithms for fringe projection profilometry: A comparative review. *Opt. Lasers Eng.* **85**, 84–103 (2016).

[9] Warnasooriya, N. & Kim, M. K. Quantitative Phase Imaging Using Multi-Wavelength Optical Phase Unwrapping. *Adv. Lasers Electro Opt.* (2010) doi:10.5772/8668.

[10] Onodera, R. & Ishii, Y. Two-wavelength interferometry that uses a Fourier-transform method. *Appl. Opt.* **37**, 7988–7994 (1998).

[11] Psota, P., Doleček, R., Lédl, V. & Vít, T. Dynamic interferometric measurement with extended unambiguity range in flow measurement. *EPJ Web Conf.* **180**, 02087 (2018).

[12] Cheng, Y.-Y. & Wyant, J. C. Two-wavelength phase shifting interferometry. *Appl. Opt.* **23**, 4539–4543 (1984).

[13] Psota, P., Cubreli, G., Kredba, J., Stasik, M. & Ledl, V. Two wavelength digital holographic interferometry for investigation of dynamic processes in fluid mechanics. in *5-6th Thermal and Fluids Engineering Conference (TFEC) - American Society of Thermal and Fluids Engineers* (Begell House Publishers, Inc., 2021).

[14] Wagner, C., Osten, W. & Seebacher, S. Direct shape measurement by digital wavefront reconstruction and multi-wavelength contouring. *Opt. Eng.* **39**, 79–85 (2000).

[15] Kreis, T. *Handbook of Holographic Interferometry: Optical and Digital Methods*. *Handbook of Holographic Interferometry: Optical and Digital Methods* (Wiley, 2004). doi:10.1002/3527604154.

[16] Chavez, S., Xiang, Q. S. & An, L. Understanding phase maps in MRI: a new cutline phase unwrapping method. *IEEE Trans. Med. Imaging* **21**, 966–977 (2002).

[17] Momose, A. Recent Advances in X-ray Phase Imaging. *Jpn. J. Appl. Phys.* **44**, 6355–6367 (2005).

[18] Pritt, M. D. Phase unwrapping by means of multigrid techniques for interferometric SAR. *IEEE Trans. Geosci. Remote Sens.* **34**, 728738 (1996).

[19] Yin, W. *et al.* High-speed three-dimensional shape measurement using geometry-constraint-based number-theoretical phase unwrapping. *Opt. Lasers Eng.* **115**, 21–31 (2019).

[20] Lu, L., Jia, Z., Luan, Y. & Xi, J. Reconstruction of isolated moving objects with high 3D frame rate based on phase shifting profilometry. *Opt. Commun.* **438**, 61–66 (2019).

[21] K, H. & F, C. Two-wavelength interferometry: extended range and accurate optical path difference analytical estimator. *J. Opt. Soc. Am. A. Opt. Image Sci. Vis.* **26**, 2503 (2009).